

Article

Sol-Gel Synthesis of New TiO₂ Ball/Activated Carbon Photocatalyst and Its Application for Degradation of Three Hormones: 17 α -EthinylEstradiol, Estrone, and β -Estradiol

El Mountassir El Mouchtari ^{1,2}, Lekbira El Mersly ¹, Kaltoum Belkodia ¹, Anne Piram ², Stéphanie Lebarillier ², Samir Briche ³, Salah Rafqah ¹ and Pascal Wong-Wah-Chung ^{2,*}

¹ Laboratoire Chimie Analytique et Moléculaire (LCAM), Faculté Polydisciplinaire de Safi, Université Cadi Ayyad, Marrakech 40000, Morocco; elmountassirelmouchtari@gmail.com (E.M.E.M.)

² Laboratoire Chimie Environnement (LCE), Centre National de la Recherche Scientifique (CNRS), Aix-Marseille University, 13000 Marseille, France

³ Département Stockage de l'Energie et Revêtements Multifonctionnels (SERM), Moroccan Foundation for Advanced Science Innovation and Research (MAScIR), Rabat 10100, Morocco

* Correspondence: pascal.wong-wah-chung@univ-amu.fr; Tel.: +33-4-13-94-98-76

Abstract: Many approaches have been investigated to eliminate pharmaceuticals in wastewater treatment plants during the last decades. However, a lack of sustainable and efficient solutions exists for the removal of hormones by advanced oxidation processes. The aim of this study was to synthesize and test new photoactive bio composites for the elimination of these molecules in wastewater effluents. The new materials were obtained from the activated carbon (AC) of *Arganian spinosa* tree nutshells and titanium tetrachloride by the sol gel method. SEM analysis allowed one to confirm the formation of TiO₂ particles homogeneously dispersed at the surface of AC with a controlled titanium dioxide mass ratio, a specific TiO₂ anatase structure, and a highly specific surface area, evidenced by ATG, XRD, and BET analysis, respectively. The obtained composites were revealed to quantitatively absorb carbamazepine (CBZ), which is used as a referred pharmaceutical, and leading to its total elimination after 40 min under irradiation with the most effective material. TiO₂ high content disfavors CBZ adsorption but improves its degradation. In the presence of the composite, three hormones (17 α -ethinylestradiol, estrone, and β -estradiol) are partially adsorbed onto the composite and totally degraded after 60 min under UV light exposure. This study constitutes a promising solution for the efficient treatment of wastewater contaminated by hormones.

Keywords: sol-gel; TiO₂; activated carbon; photocatalysis; adsorption; hormones



Citation: El Mouchtari, E.M.; El Mersly, L.; Belkodia, K.; Piram, A.; Lebarillier, S.; Briche, S.; Rafqah, S.; Wong-Wah-Chung, P. Sol-Gel Synthesis of New TiO₂ Ball/Activated Carbon Photocatalyst and Its Application for Degradation of Three Hormones: 17 α -EthinylEstradiol, Estrone, and β -Estradiol. *Toxics* **2023**, *11*, 299. <https://doi.org/10.3390/toxics11040299>

Academic Editors: Sopheak Net, Baghdad Ouddane and Giovanni Caria

Received: 28 February 2023

Revised: 17 March 2023

Accepted: 22 March 2023

Published: 24 March 2023



Copyright: © 2023 by the authors. Licensee MDPI, Basel, Switzerland. This article is an open access article distributed under the terms and conditions of the Creative Commons Attribution (CC BY) license (<https://creativecommons.org/licenses/by/4.0/>).

1. Introduction

Emerging contaminants (ECs) refer to a wide range of chemical and biological pollutants that have been recently detected in the environment and have the potential to cause adverse effects on human health and the environment [1–3]. These contaminants can arise from many sources such as industrial and agricultural activities, pharmaceuticals, personal care products, and household chemicals [4]. Their impacts on the environment can include effects on aquatic and terrestrial ecosystems, such as changes in species composition, reproductive and developmental abnormalities, and biodiversity declines. In addition, ECs can persist in the environment for long periods of time, leading to bioaccumulation and biomagnification in the food chain [5]. Estrone (E1), 17 β -Estradiol (E2), and 17 α -ethinylestradiol (EE2) are all forms of estrogen, which is a hormone primarily responsible for the development and regulation of the female reproductive system. However, estrogens also have other physiological roles in both males and females, including bone health, cognitive function, and cardiovascular health [6–9].

The concentrations of E1, E2, and EE2 in the environment can fluctuate depending on the location, source, and analysis method. However, studies have found that these

estrogens can be present in the environment at low levels, measured in nanograms per liter (ng/L). For example, in the United States, it was shown that the concentrations of E1 and E2 in river water samples ranged from less than 1 to 65 ng·L⁻¹, with an average concentration of 8 ng·L⁻¹ [4]. EE2 was detected at concentrations ranging from less than 1 to 58 ng L⁻¹, with an average concentration of 3 ng L⁻¹. In Europe, the concentrations of E1, E2, and EE2 in surface water samples are of the same order of magnitude and comprise less than 1 to 85 ng·L⁻¹, 1 to 49 ng·L⁻¹, and 0.2 to 25 ng L⁻¹, respectively [10–12]. It is important to note that even at very low concentrations, estrogens in the environment can have negative effects on aquatic wildlife, particularly fish and amphibians, which are sensitive to changes in hormone levels. Therefore, there is ongoing research and regulatory efforts aimed at reducing the discharge of estrogens into the environment and mitigating their effects [13–15].

The occurrence of organic pollutants in aquatic environments is mainly attributed to the discharge of wastewater effluents. Indeed, existing wastewater treatment plants (WWTPs) are not designed to efficiently and completely eliminate these organic pollutants [4,16]. Thus, several technologies have been developed to remove micropollutants from water and wastewater, e.g., adsorption by activated carbon [17–19], ozonation [20,21], and advanced oxidation processes (AOPs) have been developed to remove micropollutants from water and wastewater. AOPs are treatment technologies that involve the generation of highly reactive species, such as hydroxyl radicals, to degrade micropollutants. Among classical AOPs, UV/H₂O₂, Fenton's reagent, and photocatalysis with TiO₂ [22–26] can be cited, but other processes such as membrane filtration [27,28] and biological treatment [29,30] are also used. Overall, the micropollutant removal technology selection depends on several factors, including the type and concentration of micropollutants, the characteristics of the water or wastewater to be treated, and the treatment objectives. Most often, a combination of treatment technologies may be required to effectively remove micropollutants from water or wastewater. Even if some recent technologies allow for the complete removal of hormones, the formation of many by-products, sometimes more toxic than the initial one, remains questionable [31]. The use of activated carbon and TiO₂ in a composite material (AC/TiO₂) has shown promising results in removing micropollutants and their byproducts from both air and water due to the enhanced adsorption and photocatalytic capabilities of the composite material [32]. This technology is still under investigation and optimization and could be a valuable additional process to the suite of technologies available for micropollutant removal [33–36].

In line with the previous approach, the aim of this study is to propose a novel composite material made of TiO₂ and bio-sourced activated carbon for the efficient photodegradation of some pharmaceuticals, specifically hormones in wastewater under UV light irradiation. Herein, the synthesis pathway of the materials is described, as well as their characterization by SEM, XRD, BET, and ATG analysis. In addition, kinetic studies were carried out to estimate the efficiency of AC/TiO₂ composites for the removal of pharmaceutical products by both adsorption and photocatalysis and the role of TiO₂ mass ratio.

2. Materials and Methods

2.1. Chemicals

Estrone (E1), 17β-Estradiol (E2), 17 α-Ethinyl-Estradiol (EE2), and carbamazepine (CBZ) with 99% purity were provided by Sigma-Aldrich as well as titanium tetrachloride, TiCl₄, (99.99% purity), and hydrochloric acid (37%). Acetonitrile (HPLC grade), ethanol, and isopropanol (purity > 99.7%) were purchased from Fisher scientific SAS. Aqueous E1, E2, and EE2 solutions were prepared with a concentration equal to 10, 11.2, and 5.8 mg L⁻¹, respectively, and carbamazepine at 50 mg L⁻¹ with ultra-pure water from a Millipore device (Direct-Q® 5 UV, Millipore SAS, Molsheim, France) after 24 h stirring at room temperature (25 °C).

2.2. Synthesis of AC/TiO₂ Ball

Activated carbon was prepared as described in a previous work from *Arganian Spinosa* tree nutshells [36]. AC/TiO₂ ball composite materials were synthesized by the sol-gel method. For this purpose, TiCl₄ solutions (2.5, 1.29, and 0.85 M) were initially diluted in 10 mL of anhydrous isopropanol. After 5 min stirring at room temperature, 1 g of AC was added to each solution held under stirring. Then, 5 mL of distilled water was added dropwise. After 1 h of stirring at room temperature, the solvent was evaporated in a hood at room temperature and the solid was dried in the oven at 100 °C overnight.

The obtained solid materials were calcined at 500 °C in a muffle furnace for 2 h. Then, the powders were washed several times with boiling water to remove the remaining chloride ions and finally dried for 24 h at 100 °C.

2.3. Characterization of AC/TiO₂ Ball

Scanning electron microscopy (SEM) using a FEI quanta 450 FEG operating at an accelerating voltage of 200 kV allowed us to observe the morphology of composite materials. TiO₂ content in the composite was determined by thermogravimetric analysis (TGA) under air atmosphere using TGA Q5000 (TA 1000) equipment. The crystalline phase composition was determined by X-ray diffractometer using Bruker D8 Cu K α radiation ($\lambda = 1.540593$ nm) with a scan speed of 2° min⁻¹. The surface area measurements of the materials synthesized were realized using a micromeritics 3 Flex apparatus.

2.4. Photocatalysis Experiment

The photocatalytic degradation of CBZ and hormones was carried out with an irradiation setup previously used by El Mouchtari et al. [35]. The adsorption capacity of the three AC/TiO₂ ball composites was evaluated in a dark environment at 25 °C. Magnetic stirring was maintained until saturation of the material (adsorption–desorption equilibrium) for two hours. Samples were collected during the exposure at regular irradiation time. The residual concentrations were determined by high-performance liquid chromatography, and the degradation kinetics were plotted using the average data of triple experiments.

2.5. Adsorption Experiment

To determine the adsorption capacity of the composite material for CBZ, E1, E2, and EE2, we performed adsorption experiments at 25 °C. The solutions were left under magnetic stirring for 60 min to reach the adsorption–desorption equilibrium, and the equilibrium adsorption capacity Q_e (mg g⁻¹) was calculated using the following Equation 1:

$$Q_e = \frac{(C_0 - C_e) \times V}{W} \quad (1)$$

where C_e (mg L⁻¹) is the concentration of the drug product at equilibrium, C_0 (mg L⁻¹) is the initial concentration in the solution, V is the volume of the solution (L), and W is the mass of the composite material (g). The adsorption kinetics were plotted using the average data of triple experiments.

2.6. Application in Wastewaters

Wastewater was collected from Aix-en-Provence WWTP (Pioline, France), which serves 175,000 inhabitants and operates through primary and biological treatment. The collected wastewater corresponds to the final effluent after the biological treatment. The wastewater was filtered through a 0.45 μ m membrane filter using a Whatman glass microfiber filter, Binder-free GF/C 1.2 μ m, and immediately stored in the dark at -20 °C. Before starting the treatment, we determined the organic and inorganic matter in the wastewater using total organic carbon (TOC) analysis with the liquid module (Analytik, Jena, German). We found that the water contains 21.8 and 34.7 mg L⁻¹ of organic and inorganic carbon, respectively. For the irradiation experiments, the hormones were directly dissolved in wastewater effluent.

2.7. Experimental Analysis

The adsorption and degradation kinetics of hormones and CBZ were performed by HPLC (Perkin Elmer Altus 30). Chromatographic separation was obtained using a phenyl hexyl column (2.7 μm ; 2.1 \times 100 mm) distributed by the same supplier. A gradient method set at a flow rate of 0.5 mL min^{-1} and an oven temperature of 25 $^{\circ}\text{C}$. The injected volume was 5 μL . Separation was achieved using a mixture of methanol/acetonitrile (65/35) (solvent A) and water (solvent B) with the following gradient: isocratic step at 90% B for 3 min, 90% B, 90% gradient at 0% B for 8 min, and isocratic step at 0% B for 3 min. UV detection at 285, 230, 210, and 280 nm was used to detect and quantify CBZ, E1, E2, and EE2, respectively. The accuracy of the method and the quality-control approach are presented in supporting information and in Table S1. Before injection, samples were systematically filtered on a 0.2 μm cellulosic filter of 15 mm in diameter, and the non-retention of pharmaceutical compounds on filters has been tested. The filter purchased by Agilent Technologies was used to remove the photocatalyst.

3. Results

3.1. Characterization of AC/TiO₂ Ball

3.1.1. Thermogravimetric Analysis

Figure 1 shows the thermograms of AC and AC/TiO₂ ball composites with different TiCl₄ solutions. Systematically, whatever the material, two thermal events occur corresponding to two weight losses. The first one between 21 and 100 $^{\circ}\text{C}$ is probably due to the removal of water molecules adsorbed on the activated carbon surface, and the second one in the temperature range 100 to 1000 $^{\circ}\text{C}$ mainly corresponds to the combustion of carbonaceous materials.

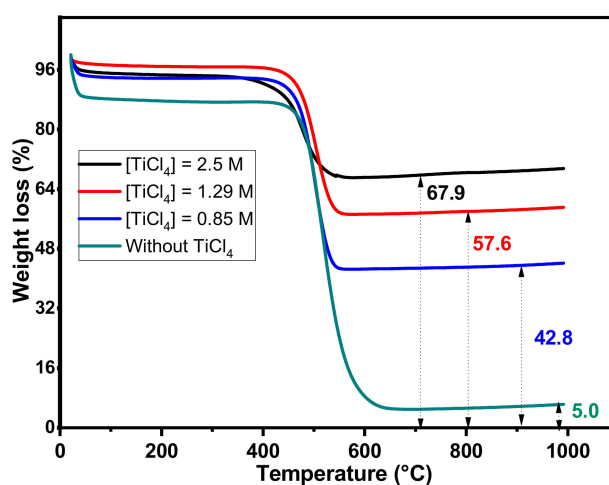


Figure 1. TGA profile of AC and AC/TiO₂ ball composites with different TiCl₄ concentrations.

The remaining weights indicated in Figure 1 suppose that almost all AC has disappeared, while the AC/TiO₂ residual part increases with the concentration of TiCl₄ solution. Consequently, it was assumed that the remaining weight in the composite corresponds to titanium dioxide formed during the sol-gel synthesis. Based on these results, the TiO₂ contents of the synthesized composites were calculated as the difference between the remaining weight of AC/TiO₂ ball and AC, and the values are gathered in Table 1.

Table 1. The theoretical and experimental mass composition (%TiO₂ theo and %TiO₂ exp), referred name, percentage of anatase and rutile structure percentage (anatase %, rutile %), and crystallite average size (TiO₂ size) as a function of TiCl₄ concentration.

[TiCl ₄] mol L ⁻¹	%TiO ₂ Theo	%TiO ₂ Exp	Referred Name	Anatase %	Rutile %	TiO ₂ Size (nm)
0.85	40.4	37.8	AC/TiO ₂ -b 38%	100	0	52
1.29	50.7	52.6	AC/TiO ₂ -b 53%	95	5	63
2.5	66.7	62.9	AC/TiO ₂ -b 63%	100	0	77

The percentages of titanium dioxide determined by ATG (%TiO₂ exp) show that the values obtained are very close to those expected (%TiO₂ theo), highlighting the ability to control the TiO₂/AC ratio by the sol-gel method as presented in Table 1.

3.1.2. Crystallography

The X-ray diffractograms of the composite materials prepared from TiCl₄ (TiO₂ mass %: 38, 53, and 63) by sol-gel method are presented in Figure 2. It is observed that regardless of the amount of TiO₂, the diffractograms exhibit similar diffraction patterns with characteristic peaks at angles of 25.18°, 36.9°, 37.86°, 48.17°, 53.83°, 55.03°, 62.64°, 68.91°, 70.25°, and 75.32°, corresponding to the reflections (011), (013), (004), (020), (015), (121), (024), (116), (220), and (125) of the anatase phase [37], respectively.

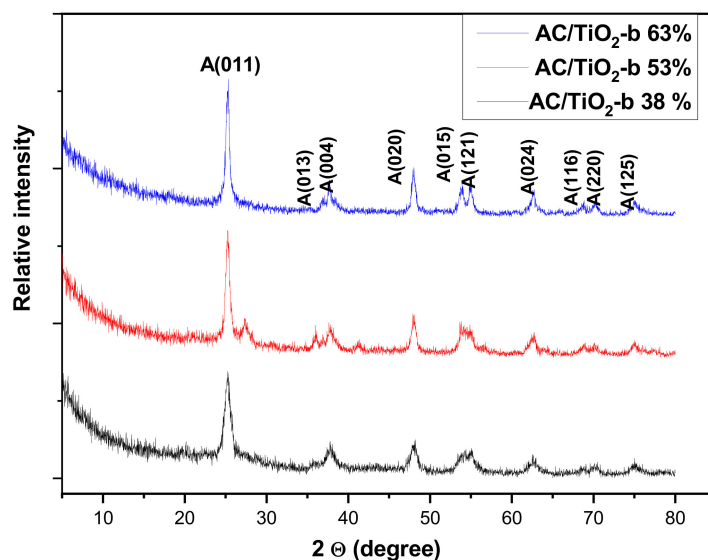


Figure 2. XRD patterns of the AC/TiO₂ ball composites.

A weak peak at 27.3° corresponding to the (110) plane of the rutile phase [38] was observed only in the AC/TiO₂-b 53% composite, which may have resulted from an unstable temperature during the calcination process at 500 °C. The classical Scherrer formula [36] was used to calculate the average crystallite size and percentage of anatase phase. The values are gathered in Table 1. From Table 1, it appears that the AC/TiO₂ composites contain predominantly TiO₂ with an anatase structure, the most photoactive one [39], and crystallites of a nanometric size around a few tenths of a nanometer on average, which help surface exchange.

3.1.3. Morphology

Figure 3 shows the morphology of activated carbon and TiO₂ composites obtained by SEM analysis with different magnifications. Figure 3a shows that the activated carbon particles have irregular shapes.

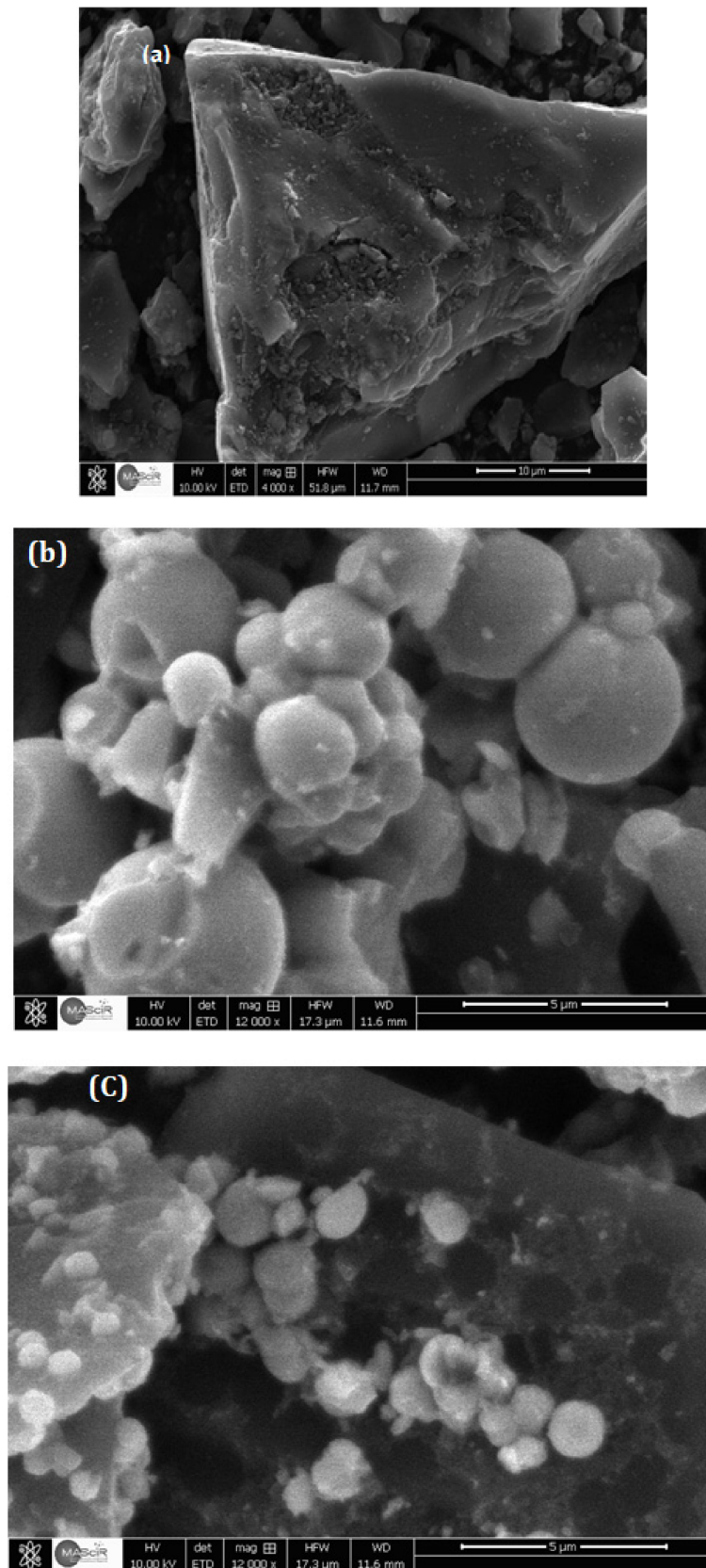


Figure 3. Cont.

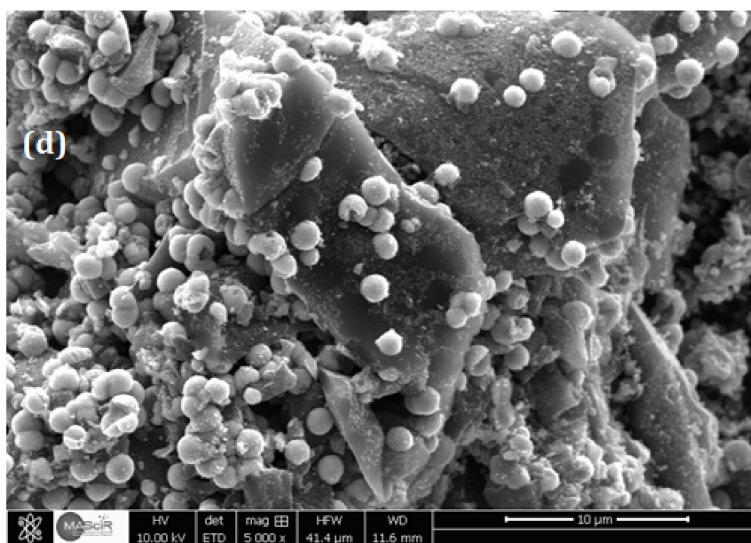


Figure 3. SEM image of AC and AC/TiO₂ ball with different magnifications: (a) AC, (b) AC/TiO₂-b 38%, (c) AC-TiO₂-b 53%, and (d) AC/TiO₂-b 63%.

On the images of AC/TiO₂-b 38% (Figure 3b), regular white beads (both solid and hollow) are observed on the surface of AC. One can also notice that grey nanobeads are deposited on the activated carbon surface for all three composites (Figure 3c).

As the TiO₂ content increases, the size of the TiO₂ particles grows and the agglomeration of white microbeads is favored, as seen in Figure 3b–d. In the same conditions, some AC surface areas contain TiO₂ nanoballs homogeneously dispersed on the activated carbon surface (Figure 3d). These observations confirm XRD analysis and validate the production of titanium dioxide beads of both a micrometric (white bead) and nanometric (grey bead) size on the AC surface carbon for all three composites with the developed synthesis protocol.

Elemental analysis of the AC/TiO₂-b 63% composites was performed by energy dispersive X-ray spectroscopy (Figure 4). The local analysis qualitatively indicates the presence of TiO₂ on the surface of AC and other elements, such as C, P, O, and N, which are constituents of the composition of AC.

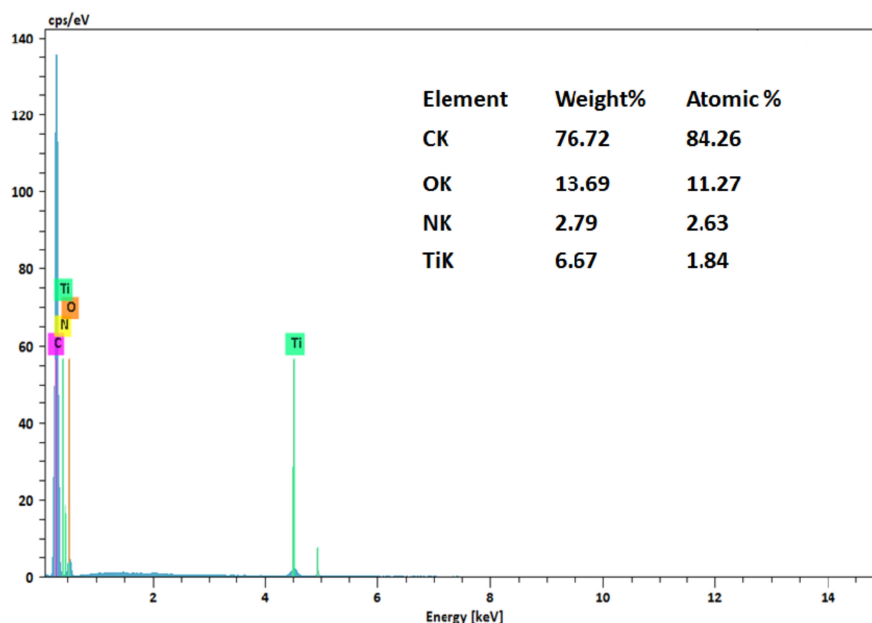


Figure 4. EDX spectrum of AC/TiO₂-b 63%.

3.1.4. Surface Area and Pore Size

The results from N₂ adsorption–desorption isotherms are presented in Figure 4 and Table 2. Figure 5 shows that the isotherms fit with type I and IV isotherms, as described in IUPAC classification [40], which are typical for materials containing micro and mesopores. Moreover, the hysteresis of the photocatalysts is very uniform, suggesting that the pores have a conical shape [41–43].

Table 2. Textural properties of AC and AC/TiO₂ composites, specific surface area (S_{BET}), porous volume, and pore diameter.

Material	S_{BET} (m ² g ^{−1})	Porous Volume (cm ³ g ^{−1})	Pores Diameter (nm)
AC	1070	0.59	2.2
AC/TiO ₂ -b 38%	736	0.43	2.4
AC/TiO ₂ -b 53%	541	0.35	2.6
AC/TiO ₂ -b 63%	422	0.28	2.7

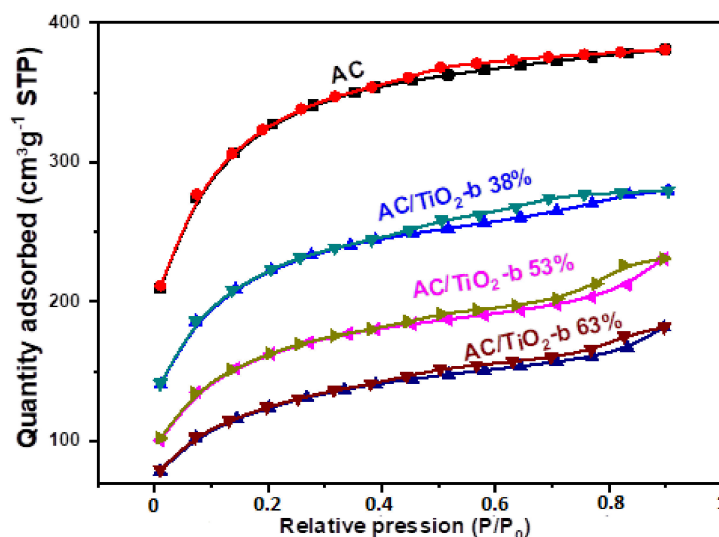


Figure 5. N₂ adsorption/desorption isotherms of AC and AC/TiO₂ composites.

Table 2 presents the textural properties of the activated carbon and composite materials. It can be observed that the addition of TiO₂ leads to a significant decrease in the specific surface area and pore volume (maximum of 60%), while the pores diameter remains almost constant.

According to DRX analysis, most of the particles are of 52 to 77 nm size average (Table 1), and the maximum of the pores diameter distribution is located around 2.2 to 2.7 nm (Table 2). Consequently, it appears difficult to conceive that TiO₂ particles can penetrate in AC pores, and this is justified by a weak change in pores diameter of the composite material compared to AC. Nevertheless, with the considered values being of an size average or maximum in diameter, an overlap of their size distribution may be possible, leading to the presence of some particles in AC large pores or their occlusion, justified by the porous volume decreases. This phenomenon is certainly negligible for small pores, and most TiO₂ particles are immobilized on the surface of the activated carbon (and few of them in the pores). Therefore, it can be concluded that the addition of TiO₂ to the composite did not significantly affect the pore nanostructure of the activated carbon.

3.2. Adsorption Equilibrium and Photodegradation Kinetic Studies

In a first approach, the efficiency of the composites has been carried out on CBZ used as a referred pharmaceutical. The effect of the contact time on CBZ adsorption reveals a two-step process as presented in Figure 6. CBZ adsorption takes place in the early stages of the experiment, and after approximately 60 min, a sorption equilibrium is reached whatever the composite. This typical adsorption profile is attributed to the large number of surface sites available at an initial time and the reduction in vacant sites on the surface for a longer contact time.

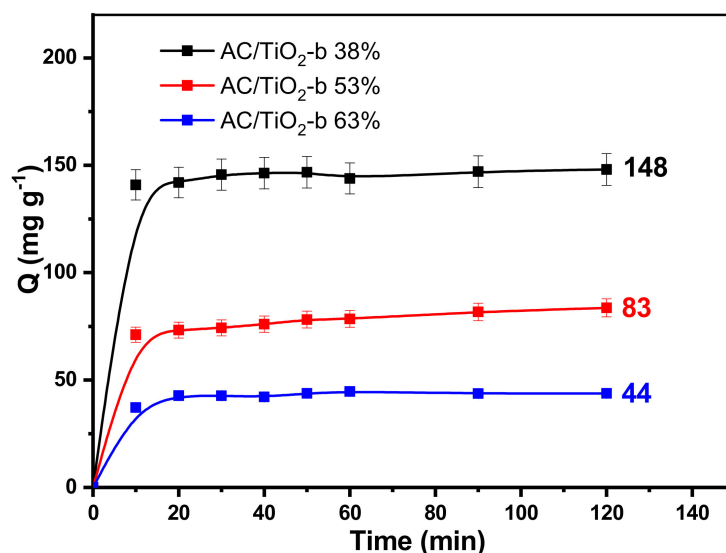


Figure 6. Concentration of CBZ adsorbed on AC/TiO₂-b as a function of time, [CBZ] = 15 mg L⁻¹, [AC/TiO₂-b] = 0.1 g L⁻¹, and T = 25 °C.

In addition, the results show that the amount of CBZ adsorbed is strongly affected by the TiO₂ amount of the material. The composite with the lowest amount of TiO₂ (AC/TiO₂-b 38%) has the highest specific surface and total pore volume and therefore exhibits the highest adsorption capacity, with a maximum amount of CBZ adsorbed (Q) around 148 mg g⁻¹. The data suggest a linear relationship between the adsorbed amount and the specific surface area as presented in Figure S1 in supporting information, in agreement with previous studies [34,36,44,45].

3.3. Photocatalytic Studies

The photocatalytic activity of the AC/TiO₂ composites was undertaken using CBZ as the model organic substrate for pharmaceuticals and because of its well-known resistant to photochemical degradation [36]. After the adsorption step, in the presence of all composites, CBZ photodegradation appears to be very effective as shown in Figure 7. However, AC/TiO₂-b 63% demonstrates a higher photocatalytic activity in comparison to the other composites since CBZ is completely removed within 40 min. The AC/TiO₂-b 53% composite allows for CBZ total disappearance in 60 min, while on the same time scale a partial elimination of CBZ is observed with AC/TiO₂-b 38%. The results suggest that TiO₂ content promotes CBZ degradation.

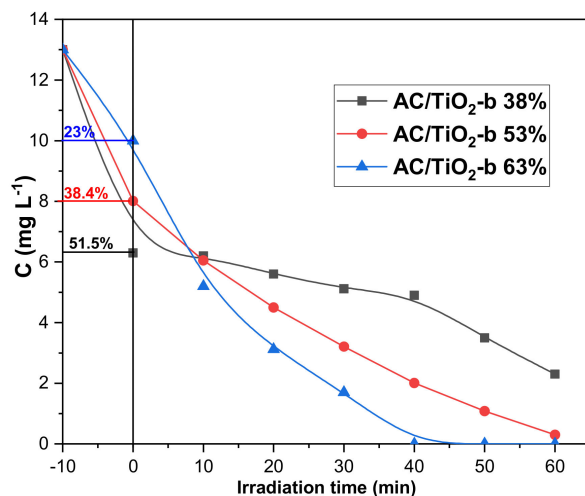


Figure 7. CBZ concentration in the presence of AC/TiO₂ ball composites as a function of irradiation time: [CBZ] = 13 mg L⁻¹, [AC/TiO₂-b] = 0.1 g L⁻¹ and Xe lamp.

3.4. Application on Wastewater Effluents

For this application, the AC/TiO₂-b 53% composite was considered as the good compromise between all composite because of its demonstrated high adsorption and photodegradation on CBZ and its reasonable amount of TiO₂, making it costly to sustain.

Assuming that the direct photodegradation of the hormones was negligible (Figure S2), their photodegradation in the presence of the composite was evaluated after stirring during 2 h in the dark to reach the adsorption/desorption equilibrium. The results of the adsorption study (Figure 8a) show that approximately, 28, 47, and 36% of E2, E1, and EE2, respectively, are removed from the effluents solution after 120 min. Thereafter, the photocatalytic degradation exhibits a high removal efficiency with a near complete disappearance of the hormones after only 60 min of irradiation time (Figure 8b).

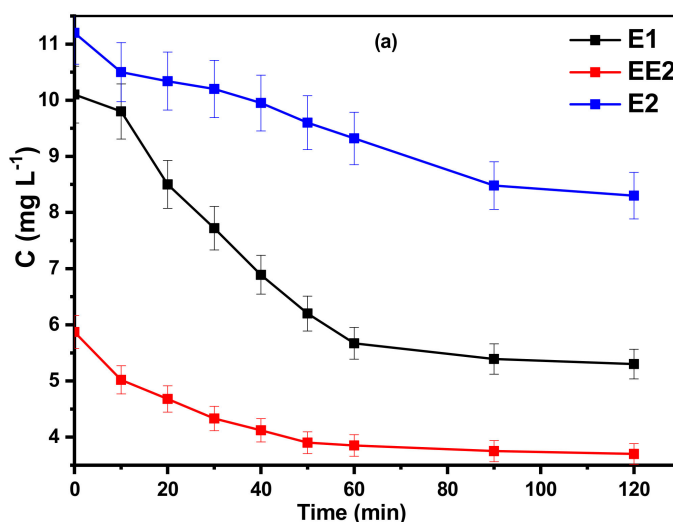


Figure 8. Cont.

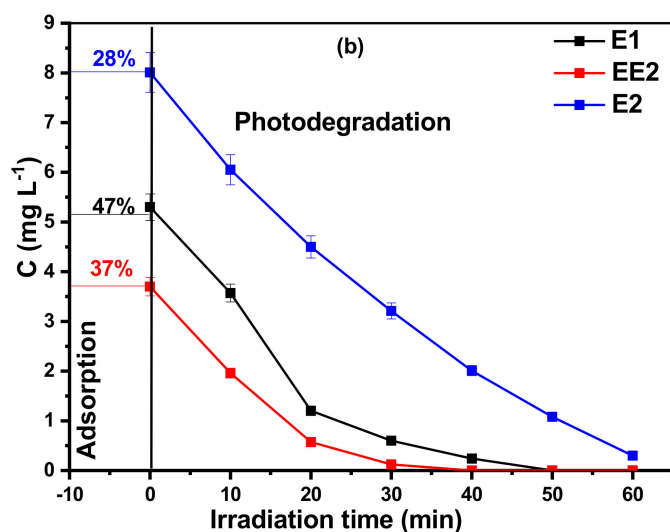


Figure 8. Hormone concentration as a function of time in the presence of AC/TiO₂-b 53% and in wastewater effluent: (a) in the dark and (b) after the adsorption step and under UV light irradiation. [AC/TiO₂-b 53%] = 0.13 g L⁻¹, [E1] = 10 mg L⁻¹, [EE2] = 5.8 mg L⁻¹ et [E2] = 11.2 mg L⁻¹, pH = 7, T = 25 °C, [O₂] = medium, Xe lamp 300 W.

The photocatalytic activity of AC/TiO₂-b 53% was compared with the reported decontamination of hormones efficiency in ultrapure and wastewater using composite materials [46–49]. Thus, in pure and ultrapure water, the partial photocatalytic degradation of EE2 was observed depending on the exposure time and material: in the presence of the CaTiO₃/WS₂ heterostructure, 91% of degradation is reached after 120 min [46], and 90% in the presence of AgCl/ZnFe₂O₄ magnetic nanocomposite after the same irradiation time [48], while only 51% of EE2 elimination is measured in the presence of ZnFe₂O₄-Ag/RGO nanocomposite after 51 min exposure [45]. In wastewater, Yang et al. reported 50% of E1 transformation by a Fenton-like process after 90 min under irradiation using biosynthesized silver nanoparticles [47]. In our work, the new material composite significantly improves the photocatalytic degradation of E1 and EE2 hormones with their total removal in 60 min in wastewater effluent. However, it is important to note that there are limited data available on the photocatalytic degradation of a mixture of hormones, and further research is needed to evaluate the effectiveness of the AC/TiO₂-b 53% composite in more complex wastewater systems. Nonetheless, these results suggest that photocatalytic degradation using the AC/TiO₂-b 53% composite could be a promising and effective solution for the removal of pharmaceutical products from wastewater.

4. Conclusions

New composite materials based on bio-sourced activated carbon and TiO₂ particles were successfully synthesized by the sol gel method using TiCl₄ with controlled TiO₂ structure, size, content, and phase. In addition, AC/TiO₂ ball materials exhibit efficient adsorption and photocatalytic degradation of the model pharmaceutical compound and of carbamazepine and allow for the total removal of hormones such as estrogens. This study highlights the potential of using AC/TiO₂ ball composites for the removal of pharmaceuticals and other emerging contaminants from wastewater, offering a promising solution for addressing water pollution and ensuring the protection of public health and the environment. Beyond the additional experiments to validate the efficiency of the process on other organic pollutants and determine optimized operational parameters, economic aspects should be studied in detail and compared to ongoing treatment in WWTP.

Supplementary Materials: The following supporting information can be downloaded at <https://www.mdpi.com/article/10.3390/toxics11040299/s1>, Table S1: Relative standard deviation (RSD, $n = 4$ for CBZ et $n = 6$ for all the hormones), limit of quantification (LOQ) and detection (LOQ) for the four pharmaceuticals by HPLC analysis, Figure S1: CBZ adsorbed concentration at sorption equilibrium as a function of specific surface area of the composite, Figure S2: Concentration of hormones as a function of irradiation time, [E1] = 10 mg L⁻¹, [EE2] = 5.8 mg L⁻¹ and [E2] = 11.2 mg L⁻¹, pH = 7, T = 25 °C, [O₂] = Medium, lamp Xe 300 W, wastewater effluent.

Author Contributions: Conceptualization, investigation, visualization, and writing—original draft, E.M.E.M., L.E.M. and K.B. Writing—original draft preparation, E.M.E.M. Writing—review and editing, E.M.E.M., P.W.-W.-C., S.R. and A.P. Data curation, methodology, S.B., S.L., L.E.M. and K.B. All authors have read and agreed to the published version of the manuscript.

Funding: This research received no external funding.

Institutional Review Board Statement: Not applicable.

Informed Consent Statement: Not applicable.

Data Availability Statement: Not applicable.

Conflicts of Interest: The authors declare no conflict of interest.

References

1. Arp, H.P.H. Emerging decontaminants. *Environ. Sci. Technol.* **2012**, *46*, 4259–4260. [[CrossRef](#)] [[PubMed](#)]
2. Hu, Y.; Yan, X.; Shen, Y.; Di, M.; Wang, J. Occurrence, behavior and risk assessment of estrogens in surface water and sediments from Hanjiang River, Central China. *Ecotoxicology* **2019**, *28*, 143–153. [[CrossRef](#)] [[PubMed](#)]
3. Diepens, N.J.; Koelmans, A.A.; Baveco, H.; van den Brink, P.J.; van den Heuvel-Greve, M.J.; Brock, T.C.M. Prospective environmental risk assessment for sediment-bound organic chemicals: A proposal for tiered effect assessment. In *Reviews of Environmental Contamination and Toxicology*; De Voogt, P., Ed.; Springer International Publishing: Cham, Switzerland, 2016; Volume 239, pp. 1–77. ISBN 978-3-319-33971-9.
4. Almazrouei, B.; Islayem, D.; Alskafi, F.; Catacutan, M.K.; Amna, R.; Nasrat, S.; Sizirici, B.; Yildiz, I. Steroid hormones in wastewater: Sources, treatments, environmental risks, and regulations. *Emerg. Contam.* **2023**, *9*, 100210. [[CrossRef](#)]
5. Tsai, H.-W.; Liao, P.-F.; Li, C.-J.; Lin, L.-T.; Wen, Z.-H.; Tsui, K.-H. High serum anti-Müllerian hormone concentrations have a negative impact on fertilization and embryo development rates. *Reprod. Biomed. Online* **2021**, *44*, 171–176. [[CrossRef](#)] [[PubMed](#)]
6. Giulivo, M.; de Alda, M.L.; Capri, E.; Barceló, D. Human exposure to endocrine disrupting compounds: Their role in reproductive systems, metabolic syndrome and breast cancer. A review. *Environ. Res.* **2016**, *151*, 251–264. [[CrossRef](#)] [[PubMed](#)]
7. Sifakis, S.; Androutopoulos, V.P.; Tsatsakis, A.M.; Spandidos, D.A. Human exposure to endocrine disrupting chemicals: Effects on the male and female reproductive systems. *Environ. Toxicol. Pharmacol.* **2017**, *51*, 56–70. [[CrossRef](#)] [[PubMed](#)]
8. Heindel, J.J.; Skalla, L.A.; Joubert, B.; Dilworth, C.H.; Gray, K.A. Review of developmental origins of health and disease publications in environmental epidemiology. *Reprod. Toxicol.* **2017**, *68*, 34–48. [[CrossRef](#)] [[PubMed](#)]
9. Rocha, M.J.; Rocha, E. Synthetic progestins in waste and surface waters: Concentrations, impacts and ecological risk. *Toxics* **2022**, *10*, 163. [[CrossRef](#)] [[PubMed](#)]
10. Loos, R.; Locoro, G.; Comero, S.; Contini, S.; Schwesig, D.; Werres, F.; Balsaa, P.; Gans, O.; Weiss, S.; Blaha, L.; et al. Pan-European survey on the occurrence of selected polar organic persistent pollutants in ground water. *Water Res.* **2010**, *44*, 4115–4126. [[CrossRef](#)] [[PubMed](#)]
11. Kolpin, D.W.; Furlong, E.; Meyer, M.; Thurman, E.M.; Zaugg, S.D.; Barber, L.B.; Buxton, H.T. Pharmaceuticals, hormones, and other organic wastewater contaminants in U.S. streams, 1999–2000: A national reconnaissance. *Environ. Sci. Technol.* **2002**, *36*, 1202–1211. [[CrossRef](#)] [[PubMed](#)]
12. Jackson, L.; Klerks, P. Effects of the synthetic estrogen 17 α -ethinylestradiol on *Heterandria formosa* populations: Does matrotrophy circumvent population collapse? *Aquat. Toxicol.* **2020**, *229*, 105659. [[CrossRef](#)] [[PubMed](#)]
13. Tyler, C.R.; Jobling, S.; Sumpter, J.P. Endocrine disruption in wildlife: A critical review of the evidence. *Crit. Rev. Toxicol.* **1998**, *28*, 319–361. [[CrossRef](#)] [[PubMed](#)]
14. Baussant, T.; Sanni, S.; Jonsson, G.; Skadsheim, A.; Børseth, J.F. Bioaccumulation of polycyclic aromatic compounds: 1. Bioconcentration in two marine species and in semipermeable membrane devices during chronic exposure to dispersed crude oil. *Environ. Toxicol. Chem.* **2001**, *20*, 1175–1184. [[CrossRef](#)]
15. Jobling, S.; Williams, R.; Johnson, A.; Taylor, A.; Gross-Sorokin, M.; Nolan, M.; Tyler, C.R.; van Aerle, R.; Santos, E.; Brighty, G. Predicted exposures to steroid estrogens in U.K. rivers correlate with widespread sexual disruption in wild fish populations. *Environ. Health Perspect.* **2006**, *114*, 32–39. [[CrossRef](#)]
16. Pessoa, G.P.; de Souza, N.C.; Vidal, C.B.; Alves, J.A.; Firmino, P.I.M.; Nascimento, R.F.; dos Santos, A.B. Occurrence and removal of estrogens in Brazilian wastewater treatment plants. *Sci. Total. Environ.* **2014**, *490*, 288–295. [[CrossRef](#)] [[PubMed](#)]

17. Zhang, A.; Luo, Y.; Jia, A.; Park, M.; Daniels, K.D.; Nie, X.; Wu, S.; Snyder, S.A. Adsorption kinetics of 20 glucocorticoids at environmentally relevant concentrations in wastewater by powdered activated carbons and development of surrogate models. *J. Water Process Eng.* **2022**, *50*, 103279. [[CrossRef](#)]
18. Yurtay, A.; Kılıç, M. Biomass-based activated carbon by flash heating as a novel preparation route and its application in high efficiency adsorption of metronidazole. *Diam. Relat. Mater.* **2023**, *131*, 109603. [[CrossRef](#)]
19. Tagliavini, M.; Weidler, P.G.; Njel, C.; Pohl, J.; Richter, D.; Böhringer, B.; Schäfer, A.I. Polymer-based spherical activated carbon-ultrafiltration (UF-PBSAC) for the adsorption of steroid hormones from water: Material characteristics and process configuration. *Water Res.* **2020**, *185*, 116249. [[CrossRef](#)]
20. Wang, C.; Lin, J.; Niu, Y.; Wang, W.; Wen, J.; Lv, L.; Liu, C.; Du, X.; Zhang, Q.; Chen, B.; et al. Impact of ozone exposure on heart rate variability and stress hormones: A randomized-crossover study. *J. Hazard. Mater.* **2021**, *421*, 126750. [[CrossRef](#)]
21. Xia, Y.; Niu, Y.; Cai, J.; Liu, C.; Meng, X.; Chen, R.; Kan, H. Personal ozone exposure and stress hormones in the hypothalamus-pituitary-adrenal and sympathetic-adrenal-medullary axes. *Environ. Int.* **2021**, *159*, 107050. [[CrossRef](#)]
22. Padovan, R.N.; de Carvalho, L.S.; Bergo, P.L.d.S.; Xavier, C.; Leitão, A.; Neto, J.D.S.; Lanças, F.M.; Azevedo, E.B. Degradation of hormones in tap water by heterogeneous solar TiO₂-photocatalysis: Optimization, degradation products identification, and estrogenic activity removal. *J. Environ. Chem. Eng.* **2021**, *9*, 106442. [[CrossRef](#)]
23. Astuti, M.P.; Rangsviek, R.; Padhye, L.P. Laboratory and pilot-scale UV, UV/H₂O₂, and granular activated carbon (GAC) treatments for simultaneous removal of five chemicals of emerging concerns (CECs) in water. *J. Water Process Eng.* **2022**, *47*, 102730. [[CrossRef](#)]
24. Antonopoulou, M. Homogeneous and heterogeneous photocatalysis for the treatment of pharmaceutical industry wastewaters: A review. *Toxics* **2022**, *10*, 539. [[CrossRef](#)]
25. Bakry, A.M.; Alamier, W.M.; Salama, R.S.; El-Shall, M.S.; Awad, F.S. Remediation of water containing phosphate using ceria nanoparticles decorated partially reduced graphene oxide (CeO₂-PRGO) composite. *Surf. Interfaces* **2022**, *31*, 102006. [[CrossRef](#)]
26. Ibrahim, A.A.; Salama, R.S.; El-Hakam, S.A.; Khder, A.S.; Ahmed, A.I. Synthesis of 12-tungstophosphoric acid supported on Zr/MCM-41 composite with excellent heterogeneous catalyst and promising adsorbent of methylene blue. *Colloids Surf. A Physicochem. Eng. Asp.* **2021**, *631*, 127753. [[CrossRef](#)]
27. Liu, S.; Véron, E.; Lotfi, S.; Fischer, K.; Schulze, A.; Schäfer, A.I. Poly(vinylidene fluoride) membrane with immobilized TiO₂ for degradation of steroid hormone micropollutants in a photocatalytic membrane reactor. *J. Hazard. Mater.* **2023**, *447*, 130832. [[CrossRef](#)]
28. Yasir, M.; Ngwabebhoh, F.A.; Šopík, T.; Ali, H.; Sedlařík, V. Electrospun polyurethane nanofibers coated with polyaniline/polyvinyl alcohol as ultrafiltration membranes for the removal of ethinylestradiol hormone micropollutant from aqueous phase. *J. Environ. Chem. Eng.* **2022**, *10*, 107811. [[CrossRef](#)]
29. Ermawati, R.; Morimura, S.; Tang, Y.; Liu, K.; Kida, K. Degradation and behavior of natural steroid hormones in cow manure waste during biological treatments and ozone oxidation. *J. Biosci. Bioeng.* **2007**, *103*, 27–31. [[CrossRef](#)]
30. Khan, K.N.; Fujishita, A.; Koshiba, A.; Mori, T.; Kuroboshi, H.; Ogi, H.; Itoh, K.; Nakashima, M.; Kitawaki, J. Biological differences between focal and diffuse adenomyosis and response to hormonal treatment. *Reprod. Biomed. Online* **2018**, *38*, 634–646. [[CrossRef](#)]
31. Rokhina, E.V.; Suri, R.P. Application of density functional theory (DFT) to study the properties and degradation of natural estrogen hormones with chemical oxidizers. *Sci. Total. Environ.* **2012**, *417–418*, 280–290. [[CrossRef](#)]
32. El Mouchtari, E.M.; Bahsis, L.; El Mersly, L.; Anane, H.; Lebarillier, S.; Piram, A.; Briche, S.; Wong-Wah-Chung, P.; Rafqah, S. Insights in the aqueous and adsorbed photocatalytic degradation of carbamazepine by a biosourced composite: Kinetics, Mechanisms and DFT calculations. *Int. J. Environ. Res.* **2021**, *15*, 135–147. [[CrossRef](#)]
33. Daou, C.; Hamade, A.; El Mouchtari, E.M.; Rafqah, S.; Piram, A.; Wong-Wah-Chung, P.; Najjar, F. Zebrafish toxicity assessment of the photocatalysis-biodegradation of diclofenac using composites of TiO₂ and activated carbon from *Argania spinosa* tree nutshells and *Pseudomonas aeruginosa*. *Environ. Sci. Pollut. Res.* **2020**, *27*, 17258–17267. [[CrossRef](#)] [[PubMed](#)]
34. Briche, S.; Derqaoui, M.; Belaiche, M.; El Mouchtari, E.M.; Wong-Wah-Chung, P.; Rafqah, S. Nanocomposite material from TiO₂ and activated carbon for the removal of pharmaceutical product sulfamethazine by combined adsorption/photocatalysis in aqueous media. *Environ. Sci. Pollut. Res.* **2020**, *27*, 25523–25534. [[CrossRef](#)] [[PubMed](#)]
35. El Mouchtari, E.M.; El Mersly, L.; Jhabli, O.; Anane, H.; Piram, A.; Briche, S.; Wong-Wah-Chung, P.; Rafqah, S. Hydrothermal synthesis of 3D cauliflower anatase TiO₂ and bio sourced activated carbon: Adsorption and photocatalytic activity in real water matrices. *Int. J. Environ. Anal. Chem.* **2022**, 1–16. [[CrossRef](#)]
36. El Mouchtari, E.M.; Daou, C.; Rafqah, S.; Najjar, F.; Anane, H.; Piram, A.; Hamadeh, A.; Briche, S.; Wong-Wah-Chung, P. TiO₂ and activated carbon of *Argania Spinosa* tree nutshells composites for the adsorption photocatalysis removal of pharmaceuticals from aqueous solution. *J. Photochem. Photobiol. A Chem.* **2019**, *388*, 112183. [[CrossRef](#)]
37. Mahmood, P.H.; Amiri, O.; Ahmed, S.S.; Hama, J.R. Simple microwave synthesis of TiO₂/NiS₂ nanocomposite and TiO₂/NiS₂/Cu nanocomposite as an efficient visible driven photocatalyst. *Ceram. Int.* **2019**, *45*, 14167–14172. [[CrossRef](#)]
38. Arthi, G.; Archana, J.; Navaneethan, M.; Ponnusamy, S.; Hayakawa, Y.; Muthamizhchelvan, C.; Ramaraj, S.G. Solvothermal synthesis of 3D hierarchical rutile TiO₂ nanostructures for efficient dye-sensitized solar cells. *Mater. Lett.* **2023**, *337*, 133961. [[CrossRef](#)]

39. Peñas-Garzón, M.; Gómez-Avilés, A.; Belver, C.; Rodríguez, J.; Bedia, J. Degradation pathways of emerging contaminants using TiO₂-activated carbon heterostructures in aqueous solution under simulated solar light. *Chem. Eng. J.* **2020**, *392*, 124867. [[CrossRef](#)]
40. Rouquerol, J.; Avnir, D.; Fairbridge, C.W.; Everett, D.H.; Haynes, J.M.; Pernicone, N.; Ramsay, J.D.F.; Sing, K.S.W.; Unger, K.K. Recommendations for the characterization of porous solids (technical report). *Pure Appl. Chem.* **1994**, *66*, 1739–1758. [[CrossRef](#)]
41. Bruschi, L.; Mistura, G.; Negri, F.; Coasne, B.; Mayamei, Y.; Lee, W. Adsorption on alumina nanopores with conical shape. *Nanoscale* **2018**, *10*, 18300–18305. [[CrossRef](#)]
42. Brunauer, S.; Emmett, P.H.; Teller, E. Adsorption of gases in multimolecular layers. *J. Am. Chem. Soc.* **1938**, *60*, 309–319. [[CrossRef](#)]
43. Asencios, Y.J.; Lourenço, V.S.; Carvalho, W.A. Removal of phenol in seawater by heterogeneous photocatalysis using activated carbon materials modified with TiO₂. *Catal. Today* **2020**, *388–389*, 247–258. [[CrossRef](#)]
44. Ribeiro, E.; Plantard, G.; Goetz, V. TiO₂ grafted activated carbon elaboration by milling: Composition effect on sorption and photocatalytic properties. *J. Photochem. Photobiol. A Chem.* **2020**, *408*, 113108. [[CrossRef](#)]
45. Abdullah, M.; Iqbal, J.; Rehman, M.S.U.; Khalid, U.; Mateen, F.; Arshad, S.N.; Al-Sehemi, A.G.; Algarni, H.; Al-Hartomy, O.A.; Fazal, T. Removal of ceftriaxone sodium antibiotic from pharmaceutical wastewater using an activated carbon based TiO₂ composite: Adsorption and photocatalytic degradation evaluation. *Chemosphere* **2023**, *317*, 137834. [[CrossRef](#)]
46. Rashki, O.; Rezaei, M.R.; Sayadi, M.H. The high photocatalytic efficiency and stability of the Z-scheme CaTiO₃/WS₂ heterostructure for photocatalytic removal of 17 α -ethinyl estradiol in aqueous solution. *J. Photochem. Photobiol. A Chem.* **2022**, *433*, 114169. [[CrossRef](#)]
47. Khadgi, N.; Li, Y.; Upreti, A.R.; Zhang, C.; Zhang, W.; Wang, Y.; Wang, D. Enhanced photocatalytic degradation of 17 α -ethinylestradiol exhibited by multifunctional ZnFe₂O₄-Ag/rGO nanocomposite under visible light. *Photochem. Photobiol.* **2016**, *92*, 238–246. [[CrossRef](#)]
48. Upreti, A.R.; Li, Y.; Khadgi, N.; Naraginti, S.; Zhang, C. Efficient visible light photocatalytic degradation of 17 α -ethinyl estradiol by a multifunctional Ag–AgCl/ZnFe₂O₄ magnetic nanocomposite. *RSC Adv.* **2016**, *6*, 32761–32769. [[CrossRef](#)]
49. Yang, K.; Liu, M.; Weng, X.; Owens, G.; Chen, Z. Fenton-like oxidation for the simultaneous removal of estrone and β -estradiol from wastewater using biosynthesized silver nanoparticles. *Sep. Purif. Technol.* **2022**, *285*, 120304. [[CrossRef](#)]

Disclaimer/Publisher’s Note: The statements, opinions and data contained in all publications are solely those of the individual author(s) and contributor(s) and not of MDPI and/or the editor(s). MDPI and/or the editor(s) disclaim responsibility for any injury to people or property resulting from any ideas, methods, instructions or products referred to in the content.